

NON DESTRUCTIVE EVALUATION OF ANISOTROPIC MEDIA WITH LASER GENERATED AND DETECTED ULTRASOUND; RECENT DEVELOPMENTS TOWARD MICROMETRIC SCALES.

B. Audoin and H. Meri,

Laboratoire de Mécanique Physique UMR CNRS 5469, Université Bordeaux 1, Bordeaux, France
b.audoin@lmp.u-bordeaux1.fr

Abstract

A method to calculate waves radiated by a nanosecond laser source through or at the surface of an anisotropic plate is discussed. Characteristic features of wave propagation in anisotropic media, such as internal diffraction are well represented. In addition, an identification method is used to measure the stiffness tensor coefficients of materials showing an orthorhombic symmetry.

Measurement of thinner layers anisotropic properties at micrometric scales with bulk ultrasonic waves requires that higher ultrasonic frequencies be excited. This can be achieved using shorter laser pulses, typically in the picosecond range. From the theoretical point of view, representation of the waves generated by such short laser pulses requires that optical and thermal material properties be considered in the calculation scheme. Calculation results of waves generated in anisotropic media are presented. Stiffnesses measurement at microscopic scale is discussed from numerical results.

Introduction

Laser generation of ultrasound is recognized to be a powerful tool to determine material properties without any contact to the sample [1]. However measurement for thin anisotropic layer requires that very high frequencies be generated. Such acoustic waves were generated with 100 fs laser pulse duration [2] and they were used to measure acoustic resonances in samples which thickness was of few nanometers only [3]. The source directivity is such that longitudinal waves are generated with a wave vector normal to the sample surface. At a mesoscopic scale, using ps laser pulses, the pupil function of the source is broadened, showing promises for the measurement of both quasi-longitudinal and quasi-shear waves.

In this paper, a model is presented to calculate the waveforms generated in any direction through an anisotropic plate. The optical penetration as well as the thermal diffusion are considered. Waveforms are calculated for a sample thickness as thin as 5 μm taking into account the source width (1 μm) and time duration (10ps).

Waveforms calculation for long (ns) laser pulses in anisotropic media

Let us first consider a silicon plate of millimetric thickness ($e = 5 \text{ mm}$). The surfaces of the plate have been cut in the plane (2,2,0) of the crystal. The normal to the interfaces of the plate, denoted axis X_1 , is along the crystallographic direction [1,1,0], while directions X_2 and X_3 belonging to the sample surface, correspond to crystallographic axes [-1,1,0] and [0,0,1], respectively. Despite the cubic symmetry of silicon, the particular orientation of the sample cut makes the wave propagation equations in the sample axes similar to those considered when propagation occurs in a material showing an orthorhombic symmetry. The components of the stiffness tensor in the sample axes can be calculated from those given by literature in the crystal axes for silicon. They are given in Tab. 1. The line-source lies in the X_3 direction thus the plane (X_1, X_2) is investigated, Fig. 1. In such a principal plane of an anisotropic material, three waves may be generated. However, since the source is a line, the shear mode which polarization is along axis X_3 is not generated for this line source direction.

We consider in this section a laser burst duration of 20 ns, and the ultrasounds are detected on the opposite face of the plate. The direction of observation is then defined by angle θ between the source-receiver direction and the plate normal, Fig. 1. The particular value $\theta = 0^\circ$ is related with the epicentre position.

The acoustic wave equation is written as:

$$\nabla \cdot (\mathbf{C}^* : \nabla \mathbf{u}) = \rho \frac{\partial^2 \mathbf{u}}{\partial t^2} = \rho T, \quad (1)$$

where \mathbf{u} and \mathbf{C}^* stand for the displacement vector and stiffness tensor, respectively. The tensor has complex components, whose imaginary parts are functions of the angular frequency ω .

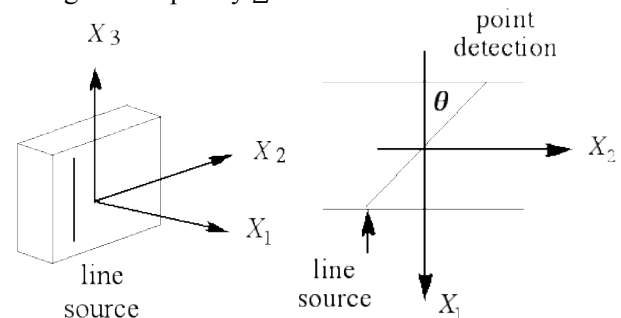


Figure 1: geometry

Any viscoelastic rheology could thus be introduced in this modelling of the displacements. However, these imaginary parts are considered null for silicon. Neglecting thermal phenomenon, the right hand side of Eq. (1) is zero.

Owing to the symmetry imposed by the source shape, the problem is invariant along direction X_3 . Each component u_i of the displacement vector depends on two space variables x_1, x_2 and on time t . The two dimension Fourier transform of the displacement field over x_2 coordinate and time t is considered, and it is noted U_i . Applying this transformation to Eq. (1) yields a set (□) of linear partial derivative equations with respect to the depth x_1 only. Classically the solution is sought in terms of exponential functions:

$$U_i = \tilde{U}_i \exp(\square j k_1^* x_1), \quad (2)$$

where k_1^* is the complex component in direction X_1 of the wave vector. Its imaginary part represents the exponential decay of the amplitude in direction X_1 .

Using Eq. (2), the set of equations (□) provides a linear system which characteristic equation is a second order polynomial form in k_1^* squared. For a given k_2 , two values of k_1^* squared can be calculated, corresponding to the propagation of modes whose polarizations are quasi-longitudinal, and quasi-transverse.

For each of the modes, the amplitudes \tilde{U}_i are calculated by expressing the boundary conditions. At $x_1 = -h$ the plate is submitted to a line loading \mathbf{F} . Since the thermoelastic regime is considered a dipole force parallel to the interface with a step-like time dependency is considered [4]. Therefore the components of \mathbf{F} are such that $F_1=0$ and $F_2 \neq 0$. The boundary conditions at $x_1 = -h$ are then expressed as follows:

$$C_{1jkl} \frac{\partial u_k}{\partial x_l} = F_j \square \delta(x_2) H(t) \text{ for } j=1..2, \quad (3)$$

where \square stands for the derivative of the delta function and H denotes Heaviside step function. Free boundary conditions are considered at $x_1 = h$, such that:

$$C_{1jkl} \frac{\partial u_k}{\partial x_l} = 0 \text{ for } j=1..2, \quad (4)$$

These four equations yield a non-homogeneous linear system for each mode. The unknowns are the components \tilde{U}_i of the two counter-propagating waves in the plate. The use of even and odd solutions uncouples this system to give two distinct systems of equations [5]. Notice that the finally considered

solutions can be either the displacement at the interface $x_1 = h$, if the transmission response is sought, or the displacement at the interface $x_1 = -h$, if the interface waves are inspected.

When dealing with an elastic medium, the integrand shows discontinuities for particular k_2 values. They correspond to poles associated with the zeroes of the dispersion equation that describe the guided waves in the plate. The integration thus appears to be not consistent with the Fourier transformation. For an accurate calculation [6,7] of the displacement field, it should be carried out in the complex plane of the variable k_2 . Since this method includes a change of variable [6] in which time interferes, it is not consistent with the frequency dependence involved by the propagation in a viscoelastic medium. A numerical integration method should therefore be applied. For each value of the angular frequency \square , the integral on the real axis of the variable k_2 is calculated by means of the method suggested by Weaver et al.[5]. In this scheme, the Fourier transform is generalized by replacing \square by a complex variable $\square - j\square$ with a small, constant and imaginary part \square . The interest of the method is twice: *i*) it preserves the applicability of the fast Fourier transform algorithms for the final inversion and *ii*) the integrand is a non-singular function that may now be integrated numerically.

A signal calculated for an angle of observation $\square = 35^\circ$ is shown in Fig. 2. For this off-epicentre detection position, the quasi-longitudinal (L) mode and the multiple arrivals of the quasi-transverse (T) mode are observed. Notice the wave with high amplitude denoted (D) in Fig. 2. It results from internal diffraction due to the folded shape of the ray curve in this anisotropic material [8].

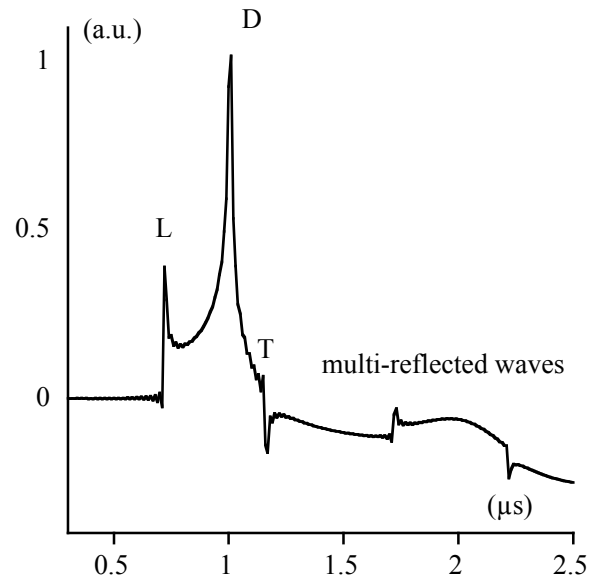


Figure 2: normal displacement for $\square = 35^\circ$ and $e = 5$ mm. The source is modelled as a dipole force at the front interface.

$C_{11} = 194.36 \text{ GPa}$	$\rho = 2.33 \text{ Kg.dm}^{-3}$
$C_{22} = 194.36 \text{ GPa}$	$\alpha = 0.15 \text{ m}^{-1}$
$C_{12} = 35.24 \text{ GPa}$	$R = 0.33$
$C_{66} = 50.90 \text{ GPa}$	$\kappa = 150 \text{ W.m}^{-1}\text{.K}^{-1}$

Table 1: physical properties of the silicon samples

Our calculations allow us to accurately represent this phenomenon. Later arrivals are also noticeable in Fig. 2 that correspond to waves propagating back and forth in the plate and reflected twice.

Measurement of stiffness coefficients

Firstly, several signals are calculated for various source to receiver directions starting at epicentre. These directions are such as they would have been obtained if either the line source or the point receiver had been scanned in a direction normal to the line with a constant step Δx . Let $(s_i(t))_N$ be the set of N calculated signals, $i = 0, \dots, N-1$. Second, the signals are shifted in time in a manner such that the waveforms calculated at two any neighbouring positions are delayed of a small constant Δt . Finally, the waveforms are summed, taking into account the symmetry of the time shift of the sources, with respect to the epicenter. It provides the signal $s(t)$ such that

$$s(t) = \sum_{i=0}^{N-1} s_i(t + \Delta t), \quad (5)$$

For suitable space sampling conditions, the obtained signal is similar to what would have been recorded if a plane wave had propagated through the material in the direction defined by angle θ .

Applying Snell-Descartes law for an acoustic source travelling along the surface with slowness $\Delta/\Delta x$, one gets access to the phase velocities for various phase directions. The stiffness coefficients can then be recovered by a numerical process starting with a set of phase velocities calculated for various phase directions [1].

Waveforms calculation for short (ps) laser pulses in anisotropic media

We now consider a sample which thickness e is $5 \mu\text{m}$, and physical properties are given in Table 1. When picosecond laser pulses are considered, the optical penetration depth can no longer be neglected and neither does the thermal diffusion length. The thermo-elastic coupling is no longer neglected in Eq. (1). It is introduced in our calculation scheme by solving Fourier diffusion equation

$$\kappa \nabla_p \frac{\partial T}{\partial t} = \nabla_{ij} \frac{\partial^2 T}{\partial x_i \partial x_j} + Q(x, t), \quad (6)$$

where ∇_{ij} are the components of the thermal conductivity tensor, whereas Q denotes the source:

$$Q(x, t) = (1 - R) I_0 \alpha(x) \exp(-\alpha x) \exp(-\kappa t), \quad (7)$$

where α stands for the absorption coefficient, R is the reflection coefficient and I_0 denotes the incident light energy. The coupled equations are solved in the (k_2, ω) Fourier domain with an appeal to the heat free and stress free boundary conditions [9].

For this $5 \mu\text{m}$ thick sample, signals were calculated for an angle of observation $\theta = 35^\circ$. The signal calculated taking into account thermal diffusion and optical penetration depth is plotted in Fig. 3 along with the signal calculated when a dipole source on the surface is considered, Eq. (3). For this off-epicentre detection position, the quasi-longitudinal (L) mode, the quasi-transverse (T) mode and the wave resulting of internal diffraction (D) are still clearly observed. When optical penetration is considered, thermal sources of expansion are on a plane normal to the plate interface and containing the laser line source. Since the optical penetration depth $(1/\alpha)$ is higher than the sample thickness, an additional wave denoted (Ls), is observed in Fig. 3, before the (L) wave.

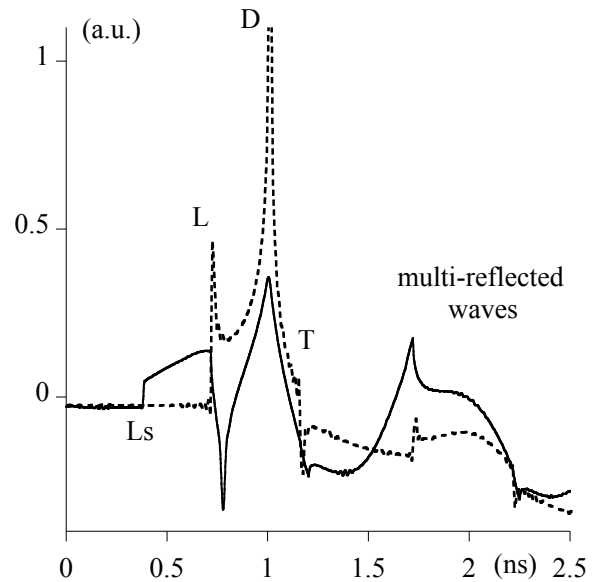


Figure 3: normal displacement for $\theta = 35^\circ$ and $e = 5 \mu\text{m}$. Dashed line was calculated for a dipole force at the front interface. Solid line was calculated taking into account both optical penetration and thermal diffusion.

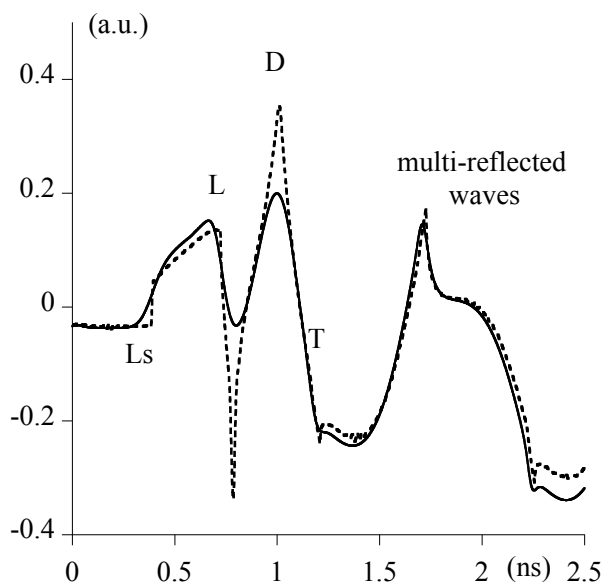


Figure 4: normal displacement for $\theta=35^\circ$ and $e = 5 \mu\text{m}$. Dashed line was calculated taking into account both optical penetration and thermal diffusion. Source width and time duration were also accounted for to plot the solid curve.

It corresponds to a longitudinal skimming wave, propagating from the epicentre to the detection point. In addition to the correct representation of the generation mechanism, one must also take into account the source characteristics in time and space. To this aim, the delta functions $\delta(x_2)$ and $\delta(t)$ in Eq. (7) are changed in Gauss functions which width at mid height equal the pulse width and pulse duration, respectively. The obtained signal is shown in solid lines in Fig. 4 with the signal already discussed in Fig. 3. When the laser beam properties are considered, the signal is smoothed owing to the convolutions with Gauss functions in space and time domain. However, for realistic $1\mu\text{m}$ width and 10 ps duration, the shear wave (T) is still easily discernable in the waveform, as well as the wave resulting of internal diffraction (D), which is a signature of anisotropy.

Conclusion

In this paper a model is considered to calculate acoustic waves generated by short laser pulses (ps) for which optical penetration and thermal diffusion can no longer be neglected. Moreover, pulse properties such as time duration and width are also considered. A typical waveform for a point detection located on the opposite side of a $5\mu\text{m}$ thick plate at an off-epicentre position was calculated. A laser pulse of 10 ps is considered and a source width of $1\mu\text{m}$ is assumed. The calculation shows that the shear wave is still clearly discernable. This result shows promises for the non-destructive evaluation of thin films.

References

- [1] F. Reverdy and B. Audoin, "Elastic constants determination of anisotropic materials from phase velocities of acoustic waves generated and detected by lasers," *J. Acoust. Soc. Am.*, **109**(5), pp. 1965-1972, 2001.
- [2] C. Thomsen et al., "Coherent phonon generation and detection by picosecond light pulses", *Phys. Rev. Lett.*, **53**(10), 989-992, 1984.
- [3] B. Perrin et al., "Picosecond ultrasonics study of metallic multilayers", *Phys. B*, **219&220**, 681-683, 1996.
- [4] L. R. F. Rose, "Point-source representation for laser-generated ultrasound" *J. Acoust. Soc. Am.* **75**, 723-732, 1984.
- [5] R.L. Weaver, W. Sachse, and K.Y. Kim, "Transient elastic waves in a transversely isotropic plate", *J. Appl. Mech.* **63**, 337-346, 1996.
- [6] A.T. De Hoop, "A modification of Cagniard's method for solving seismic pulse problem", *Appl. sci. res.* **B-8**, 349-356, 1960.
- [7] A. Mourad, et al., "Acoustic waves generated by a transient line source in an anisotropic half space", *Acta Acustica* **52**, 839-851, 1996.
- [8] H.J. Maris, "Effect of finite phonon wavelength on phonon focusing", *Phys. rev. B.*, **28**(12), 7033-7037, 1983.
- [9] M. Dubois et al., "Modeling of laser thermoelastic generation of ultrasound in an orthotropic medium", *Appl. Phys. Lett.*, **64**(5), 554-556, 1994.